Static Analysis of Prestressed Floor Slabs HC500 with Changes in Tendon Adhesion to Concrete Induced by Penetration of Chloride Ions

Static Analysis of Prestressed Floor Slabs HC500 with Changes in Tendon Adhesion to Concrete Induced by Penetration of Chloride Ions

Zofia Szweda [1] Radoslaw Jasinski [1]

[1] Department of Building Structures, Silesian University of Technology, Akademicka 5, 44-100 Gliwice, Poland

zofia.szweda@polsl.pl

Abstract. Prestressed hollow-core slabs are suitable for various span applications in different types of buildings. Such structures are quick to mount and do not require boarding system or assembly supports reducing deflection, which is an economic asset. The performed analysis included HC-500 slabs made of C50/60 concrete with w/c ratio of 0.31, with Portland cement CEM II 52.5 R. Strength of such structures is determined by, among other things, chloride ion concentration at the interface between the surface of prestressing tendons and concrete. Corrosion products, induced by chloride ions, will certainly reduce stress of adhesion to concrete, and consequently, second-order momentum in the structure. It may be difficult to draw firm conclusions about the predicted strength of analysed slabs on the basis of the obtained results. Therefore, we performed the static analysis including the changes in tendon adhesion to concrete caused by corrosion. We also analysed the bearing capacity of slabs according to concrete cover thickness of upper and lower tendons. The analyses included results from the accelerated tests on chloride ion penetration to cylindrical elements drilled directly from the top surface of prefabricated prestressed floor slabs HC500-19/R120. Those results were used to determine the diffusion coefficient of chloride ions into concrete, from which the analysed slabs were made. The value of diffusion coefficient $\overline{D}_{s}^{1} = 0.72 \cdot 10^{-12}$ m²/s for the tested concrete was used to illustrate results for changes in the bearing capacity over time. We determined times, after which those tendons could corrode, assuming that penetration of chloride ions is observed only at the surface of the upper floor slab. The obtained results were used to develop recommendations and draw conclusions for further tests.

1. Introduction

Assembly of such structures is quick and does not require a boarding system or supports to reduce deflection, which is an economic asset [1]. The analysis was performed on HC-500 slabs made of C50/60 concrete with w/c ratio of 0.31, based on Portland cement CEM II 52.5 R. Strength of such structures is determined by, among other things, chloride ion concentration at the surface of prestressing tendons in contact with concrete. Products of corrosion, which was induced by chloride ions, can certainly reduce bond stress to concrete, and consequently, reduce 2nd order moment in the structure [2, 3]. High strength prestressing steels show a far more sensitive reaction to a corrosion attack than reinforcing steels, which can be observed in the following sequence of tests: tensile test - fatigue test – stress corrosion test. In case of an uneven local corrosion, a corrosion depth of 0.6 mm may suffice for breaking a cold deformed wire under tension of 70 % of the specified tendon strength of about 1800 N/mm^2. At the pitting depth

of above 0.2 mm, cold drawn wires may show fatigue limits (fatigue limits for stress cycles of N = $2 \cdot 10^6$) of 100 N/mm^2 and less. Like-new smooth surfaced steels normally show a fatigue limit of more than 400 N/mm^2. The problem of corrosion fatigue cracking of cracked components can be remedied by providing a sufficient concrete cover and limiting the crack width. This is the way of keeping pollutants away from the prestressing steel surface. A cold drawn prestressing steel wire shows a decrease of the corrosion fatigue limit in the sequence air-water-chloride solution. For frequencies of 0.5 s^{-1}, the fatigue limit for stress cycles of 10^7 is below 100 N/mm^2 [2]. It was found that reduction factors for yield and ultimate stresses of the naturally corroded bars were similar to those of the artificially corroded bars. However, the reduction factor for the ultimate strain of the naturally corroded bars was much smaller than that of the artificially corroded bars. This suggests that the distribution of the cross-sectional areas was more non-uniform in artificially corroded bars than in naturally corroded bars. It is more appropriate to use the impressed-current method on bars embedded in concrete than on bare bars to simulate natural corrosion caused by a chloride attack. [3]. In the constant corrosive condition of accelerated corrosion test [4], with an increasing prestressing level, corrosion velocity also increased to 124.3 – 126.5% for 20% level, 165.5 – 166.8% for 40% level, and 178.5 – 189.8% for 60% level of prestressing with a clear linearity relation. With increasing prestressing level, clear reduction of ultimate strength and elongation to break are observed; however, the stiffness degradation is not evaluated clearly due to twisted shape and local corrosion of tendon.

Whilst considerable research has been undertaken on steel corrosion in concrete, it is more focused on reinforcing steel than on prestressing steel. Although the underlying corrosion science is the same for both steels, the applicability of data on corrosion obtained from reinforcing steel to prestressing steel needs proof due to primarily the mechanical and physical differences between the two, in particular, the high level of stresses in prestressing steel strands and the microstructure of prestressing steel strands. As shown in Figure 1, there are fewer corrosion cells on the surface of prestressing strands than that of deformed bars. This reduced number of corrosion cells leads to faster growth of local corrosion at already corroded spots (cells). Since there is relatively more supply and less demand of water and oxygen for a small number of corrosion cells to sustain, pitting corrosion dominates in each strand (wire). Therefore, for corroded strands, more local and uneven corrosions occur as shown in Figure 1 [5].

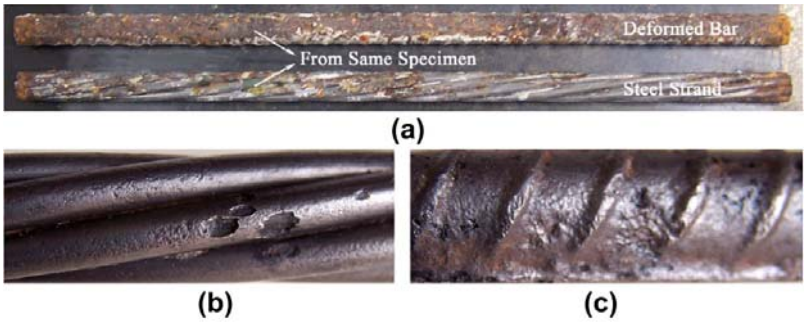

Figure 1. Corrosion characteristics of: (a) strand and bar, (b) details of strand, (c) details of bar [5]

From the analysis of the ultimate bond stress of all the specimens before, it can be seen that the presence of fatigue does improve the ultimate bond strength of the specimen, but this improvement is not infinite. When the fatigue accumulates to a certain extent, the ultimate adhesion of the specimen will be degraded [6].

Corrosion of the strand in a pre-tensioned prestressed concrete structure was found to degrade the tensile strength of the strand instead of its bond strength. The experimental investigation into the tensile behaviour of corroded strands presents an approximately linear degradation law for the tensile strength of strands with the corrosion rate.

The fitting model is shown in the following formula:

$$f_{ptm,c}=(1.00\text{-}3.41\,\eta)\cdot f_{ptm,0} \quad (1)$$

where f_{ptm} and $f_{ptm,0}$ are the tensile strength of corroded and uncorroded strands, respectively, and η is the corrosion rate. The corrosion rate ranges from 1.73% to 2.87%, but the corrosion crack does not appear. Thus, the corrosion rate corresponding to the critical crack width of 0.6 mm exceeds 2.87%, and accordingly, the degradation in tensile strength of the corroded strand exceeds 9.8%. When the bond strength of the corroded strand begins to degenerate, the tensile strength degenerates by more than approximately 10%, which may lead to a serious structural failure. Thus, the effects of strand corrosion on pre-tensioned prestressed concrete structures is evident mainly in the degradation of tensile strength rather than in the degradation of bond strength. [7].

In general, values of corrosion rates higher than 10 μA/cm^2 are seldom measured while values between 0.01 and 1 μA/cm^2 are the most frequent. When the steel is passive, very low values (smaller than 0.05–0.1 μA/cm^2) are recorded. These current density values can be translated into a loss in diameter applying the Faraday law, thus a corrosion rate of 1 μA/cm^2 produces a section reduction of 10 μm per year. When the corrosion rate is presented as μm/year, it is named V_{corr} instead of I_{corr}. The accumulated corrosion is termed corrosion penetration, P_x, and can be expressed as a loss in diameter $\phi_t = (\phi_0 - 2P_x)$ with ϕ_t being the diameter after time t and ϕ_0 = the initial diameter.

This reduced diameter can be due to localized (P_{pit}) or homogeneous corrosion, as Figure 2 illustrates. It has been established that P_{pit} can be calculated from P_x as there is a relation between the homogenous corrosion penetration and the maximum depth of a pit. This relation is named pit factor, α, which usually ranges between 3 and 15, with 10 being a suggested averaged value [8].

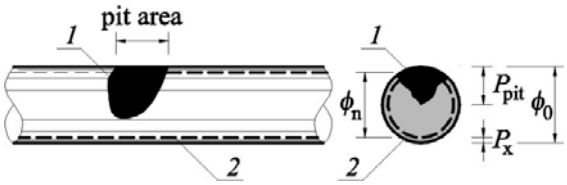

Figure 2. Homogeneous or uniform corrosion equivalent to a localized corrosion showing a single pit with a corrosion depth of P_{pit} [8]: *1* – localized corrosion, *2* – equivalent uniform corrosion

Average corrosion rates V_{corr} = 30 μm/year are given for the exposure classes XD2 or XD3 of EN206 [9].

The bond strength [10] was determined from the bar force over the anchorage area. At each corrosion level, the estimated bond strength (peak value) was normalized by the square root of the 28-day compressive strength f'_c of the slab concrete, following familiar ACI Code practice. Normalized values of bond strength (MPa) were plotted against the percentage of mass loss for all specimens. Accumulation of the corrosion product had only the effect to increase tension in the concrete zone surrounding the bar, thereby accelerating the process of bond degradation. The mean predictor equation developed was

$$\frac{f_{bpt}}{\sqrt{f_c'}} = 0.77 - 0.027xr^2 \quad (2)$$

where f_{bpt} is the bond strength in MPa, and x is the percent of mass loss of steel bar in the end regions. The variable x is defined as

$$x = \frac{m_n}{m_0} \cdot 100\% = \frac{V_n}{V_0} \cdot 100\% \tag{3}$$

where m and V are the mass and volume in the end regions, respectively, and the subscript 0 refers to the initial stage and n refers to the new, corroded stage. Note that the normalized bond strength of the uncorroded slabs tested herein was 0.75. Also, to express bond deterioration in terms of residual bar diameter, Eq. (3) is reduced to

$$x = \left(1 - \frac{\phi_n^2}{\phi_0^2}\right) \cdot 100\% \cong 2\frac{\Delta\phi}{\phi_0} \cdot 100\% \tag{4}$$

where D is the diameter of the bar. Substituting Eq. (2) into Eq. (4) the normalized residual bond strength is calculated as

$$\frac{f_{bpt}}{\sqrt{f_c'}} = 0.77 - 2.7\left(1 - \frac{\phi_n^2}{\phi_0^2}\right) \cong 0.75 - 5.4\frac{\Delta\phi_n}{\phi_0} \tag{5}$$

It may be difficult to draw firm conclusions about the predicted strength of analysed slabs on the basis of the obtained results [11]. Therefore, we performed the static analysis including the changes in tendon adhesion to concrete caused by corrosion. We also analysed bearing capacity of slabs according to concrete cover thickness of upper and lower tendons. The analyses included results from the accelerated tests [11] on chloride ion penetration to cylindrical elements drilled directly from the top surface of prefabricated prestressed floor slabs HC500-19/R120. Those results were used to determine diffusion coefficient of chloride ions into concrete, from which the analysed slabs were made. The value of diffusion coefficient $\overline{D}_s^1 = 0{,}72 \cdot 10^{-12}$ m^2/s for the tested concrete was used to illustrate the results for changes in bearing capacity over time. We determined times, after which those tendons could corrode assuming that penetration of chloride ions is observed only at the surface of the upper floor slab. The obtained results were used to develop recommendations and draw conclusions for further tests.

2. Protective properties of concrete cover in prestressed floor slabs HC500

The test described in [11] was performed on elements drilled directly from the top surface of precast prestressed floor slabs HC-500, using a diamond drilling machine - Figure 2 (left). Considered precast concrete with w/c = 0.32 and average compressive strength of concrete f_{ctm} = 65 MPa was made of C50/C60 concrete, based on Portland cement CEM II 52.5 R 550 kg/m^3 and Crushed BASALT: 1304 kg/m^3 [12].

The test was [11] carried out on six cylindrical specimens with a diameter of 8 cm and height of 50 mm, whose side surfaces were coated with resin to ensure unidirectional flow of chloride ions. Containers with 3% NaCl solution were attached firmly to the top surface of cylindrical specimens. Stainless steel cathodes with a size adjusted to cross section of cylindrical elements, were placed inside the containers. The tests were simultaneously performed on three specimens connected in parallel to form the electric circuit - Figure 2 (right). Chloride ions migrate in concrete through liquid present in pores containing dissolved components of hydrated cement. We used the thermodynamic model of chloride ingress in concrete described in the paper [14] to analyse ion flow in pore solution. We identified a theoretical representative of volume X - Figure 2 (right), and then defined concrete structure with water-filled pore space as an inert component $\alpha = 0$ which was not directly involved in the process. The following anions $Cl^- - \alpha = 1$, $OH^- - \alpha = 2$ and cations $Na^+ - \alpha = 3$, $K^+ - \alpha = 4$ and $Ca^{2+} - \alpha = 5$ were the components involved into this process.

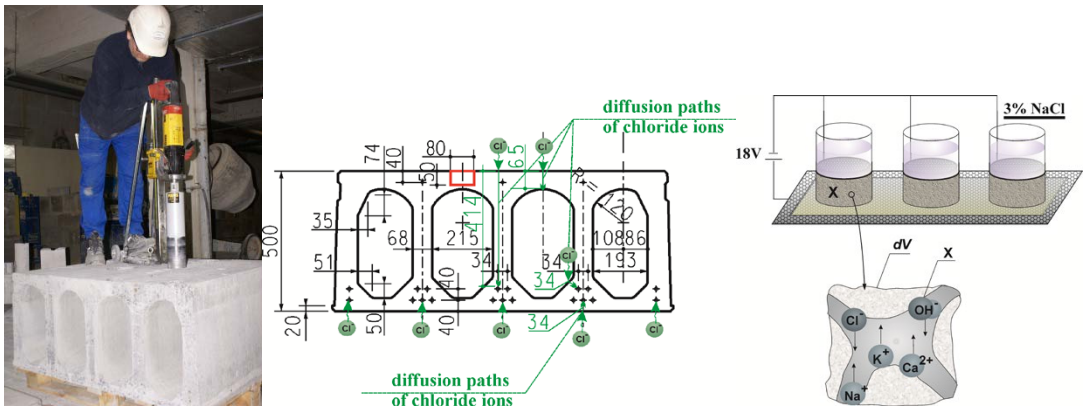

Figure 3. (left) Elements drilled directly from the top surface of precast prestressed floor slabs HC-500, using a diamond drilling machine. (right) The model of ion ingress in concrete: a) electrical scheme, b) the process components in the representative volume element, c) Diffusion path of chloride ions

The specimens, after being soaked in distilled water for 72 hours to increase electrical conductivity of concrete, were placed on a wet sponge with a platinum-plated titanium mesh anode underneath. Then, a set of specimens was connected to a direct current supply with voltage U = 18 V. The tests on chloride migration were performed for two times t_1 = 24 and t_2 = 48 hours. NaCl solution was replaced after 24 hours. During the whole period of tests, the temperature of solution was constant, at about 20°C. When the migration process was completed, the specimens were left under ambient conditions for 72 hours. Concrete powder was collected from each specimen, from 10 consecutive depth increments of thickness g = 2 mm using "Profile Grinding Kit" from German Instruments AS company. We aggregated powder concrete from three similar specimens and added distilled water in a 1:1 weight ratio. That dense solution was stirred every few hours per 24 hours, and then passed through a medium-sized filter. Washing out was repeated twice. The experimental solutions were subjected to a chemical analysis to determine concentration c^1 [mg/dm^3] of chloride ions in the liquid by argentometric titration in accordance with the Mohr's method (standard ISO 9297) [13]. Water weight by volume γ_w= 1 kg/dm^3 was used to estimate volume V_r of the experimental liquid, and then to determine mass density ρ^1 of chloride ions [15].

On the basis of measured mass distribution ρ^1 of chloride ions migrating in concrete under the electric field, the value of diffusion coefficient $\overline{D}\,_s^1 = 0{,}72 \cdot 10^{-12}$ was obtained for the steady state of the tested concrete classified the tested concrete to the group with a very low chloride permeability [14-16].

Protective properties of concrete cover were determined by calculating an increase of chloride ion concentration from experimentally determined diffusion coefficient. For calculations, concrete cover c_{nom} = 35 mm was used for tendons Ø9.3 made of steel Y1860, typical for those hollow-core slabs. The tendons formed the top reinforcement protecting concrete on the top surface of prefabricated units against cracking in the initial stage, directly after compression, and they protected long slabs against breaking down while they were lifted. Additionally, the cover c_{nom} = 55 mm was determined according to Table 4.5N, EN 1992-1-1 [17] assuming the structure durability (50 years) for structural class S4 and exposure class XD3 – cyclic wet and dry environment, parts of bridges exposed to spray containing chlorides, pavements, car park slabs. According to EN 1992-1-1 [17], prestressing tendons in the top part of a slab were prone to corrosion induced by chloride ions reaching the critical concentration C_K = 0.2% by cement mass. We also determined the shortest path of chloride ion ingress in prestressing tendons with a diameter Ø12.5 located in the bottom part of a slab. That path was a sum of thickness of a top slab in the structural-floor tile - 65 mm and a tendon cover at the inner side of the hollow core - 34 mm. Corrosion risk for tendons in the bottom part of main reinforcement was assumed to be induced by a critical concentration of chloride ions equal to 0.1% according to EN 1992-

1-1 Eurocode 2 [17]. Changes in chloride concentration over time t were computed according to the known solution for diffusion equation [14, 16, 19]. These changes are illustrated in Figure 4.

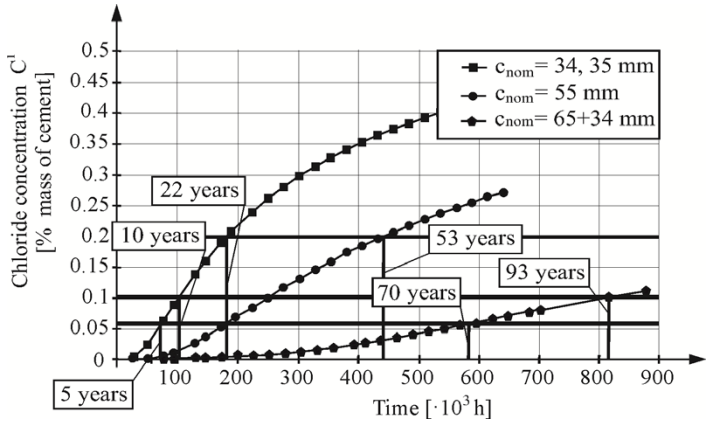

Figure 4. Time-dependent changes of chloride concentration in concrete-steel contact zone for three different thickness values (34, 35, 55 and 99 mm) of concrete coatings of steel prestressing tendons

They referred to the interface between prestressing tendons in the top part of concrete and concrete cover - 35 mm and 55 mm, respectively, and for the shortest determined path of chloride ingress in lower edges of prestressing tendons in the main reinforcement – 99 mm. Time, after which prestressing tendons were prone to corrosion, was specified by comparing chloride concentration to the critical value. Corrosion risk for top tendons will appear after 22 years of the structure operation providing that cover thickness is 35 mm. The minimum thickness of the cover for top tendons for structural class S4 and exposure class XD3, that is, the thickness of 55 mm would protect upper tendons against corrosion for 53 years. Assuming that chloride ions penetrate bottom tendons from the top surface of floor slab, and the limit value of chloride concentration is C_K = 0.1%, corrosion of tendons is possible after 93 years of operation. For the limit value of chloride concentration C_K = 0.06, bottom tendons will corrode after 70 years. And assuming that chloride ions can reach the bottom surface of the reinforcement tendons, they can also reach the top edge of the tendon in case of steam or careless sealing of the end of the structural-floor tile. For the edge of first bottom or top tendon, ultimate concentration can be calculated as C_K = 0.2% after 20 years. If the cover thickness is 34 mm, the value can reach C_K = 0.1% after 10 years, and C_k = 0.01 after only 5 years.

It may be difficult to draw firm conclusions about the predicted strength of analysed slabs on the basis of the obtained results [11]. Therefore, we performed the static analysis including the changes in tendon adhesion to concrete caused by corrosion.

3. Static analysis including the changes in tendon adhesion to concrete caused by corrosion

The controlled transmission of forces on concrete is the fundamental aspect of the prestressed structures. In the prestressed structures, tendons bonded to concrete become particularly important. Design stresses at the side surface of prestressing tendons are lower than the design resistance $\tau_p \leq f_{bpt}$. Due to obvious reasons, the anchorage zone of the prestressing tendons is verified. However, adhesion is assumed in the relevant sections in terms of bending. The design simulation for the slab HC-500 having the structure as shown in Figure 5 was run to explain the effect of changes in bond strength. For the design purpose, it was assumed that the total length of the slab was L = 13 m, theoretical span was l_{eff} = 12.85 m. Apart from self-weight of the slab (g_k=7.34 kN/m), the additional constant load resulting from weight of concrete over-layer and layers of floor, (Δg_k=5.11 kN/m) and variable load (q_k = 6.00 kN/m) were assumed. Nineteen prestressing tendons with 7-wire strands, and diameter of 12.5 mm, made of steel grade Y 1860, 2 relaxation class, were used in central ribs of the slab. Reinforcement in the top ribs was composed of two tendons with 7-wire strands, a diameter of 9.3 mm, made of steel grade Y. According

to [12], the slabs were prepared on a casting bed with the length of 100 m and cured for 2 days. After 7 days, bottom tendons were prestressed with the overall force equal to $P_1 = 19 \times 93 = 1767$ kN and the top ones with the force $P_2 = 2 \times 56 = 112$ kN.

Functionality of prestressed elements is determined by concrete properties, changes in the prestressing force over time, and possible corrosion losses for steel. The authors' own tests on the effect of Cl^- ions described under point 2 revealed local points of corrosion and pitting effects in the strands. And the tests [10] confirmed the noticeable effect of the aggressive environment on the strength of strand bonding to concrete.

To evaluate the effect of Cl^- ions, the following assumptions were made:

a) the effect of aggressive environment would be observed after time $t_{ini.cor}$, during which chloride ions would penetrate the cover of prestressing tendons, and then the whole group of tendons after the t_n time,
b) bond stress would change over time in accordance with the expression (4). Lower bond strength between concrete and tendons would reduce the strength of tendons, and the additional delayed loss ΔP_{cor} – Figure 6, would be assumed,
c) corrosion would reduce the area of prestressing tendons. The prestressing force would remain unchanged, but there would be an increase in tensile stresses in the sections impaired by pitting.

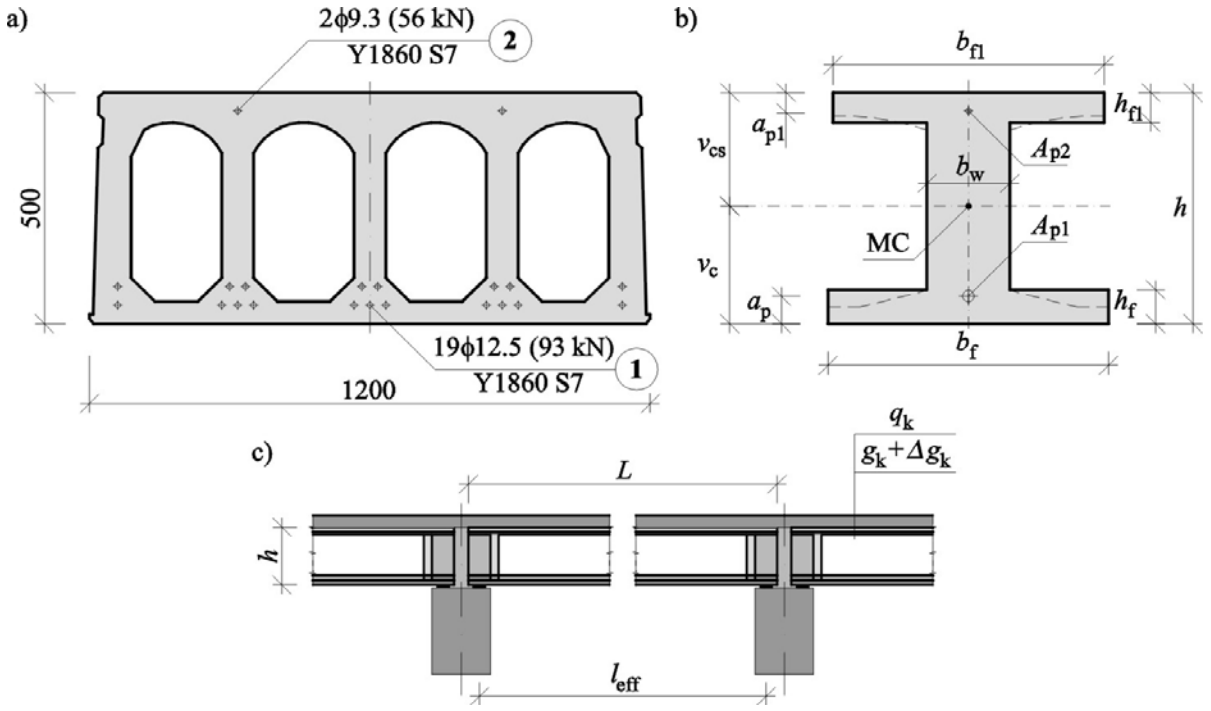

Figure 5. Geometric parameters of the slab applied in the calculations: a) cross section, b) design section, c) longitudinal section

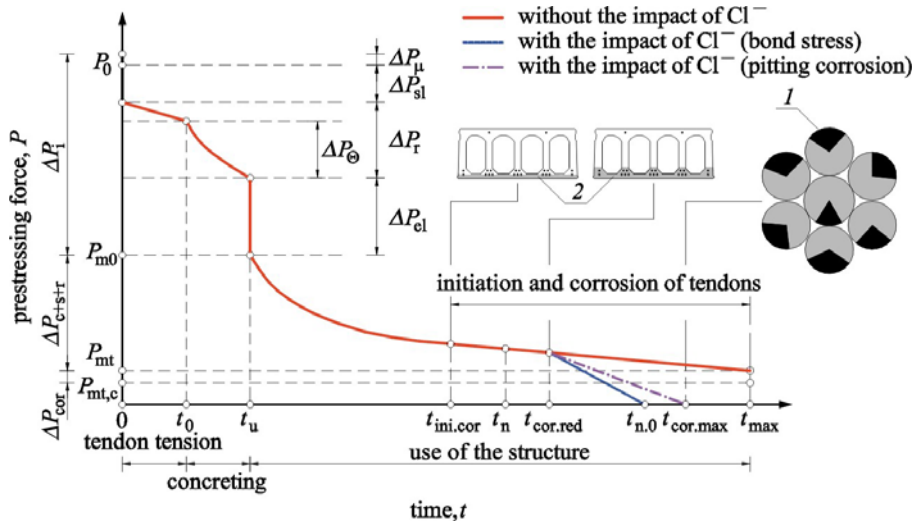

Figure 6. Prestressing losses in prestressed concrete elements: 1 – revealed local points of corrosion and pitting effects in the strands, 2 –zone of contamination of concrete chlorides

To calculate the component ΔP_{cor} of losses in the prestressing force, the time of corrosion initiation was taken as $t_{ini.cor}$=22 years, bond stresses after time $t < t_{ini.cor}$ were taken as

$$f_{bpt}\left(t \le t_{ini.cor}\right) = \eta_{p1}\eta_1 f_{ctd}\left(t\right), \tag{6}$$

bond stresses after the time of corrosion initiation are expressed by the following formula

$$f_{bpt}\left(t > t_{ini.cor}\right) = \sqrt{f_c'(t)}\left(0.75 - 5.4\frac{\alpha\eta V_{corr}(t)}{100\phi_0}\right), \tag{7}$$

where:

η_{p2} = 1,2 – 7-wire strands,
η_1= 1,0 – satisfactory bonding
f'_c – 28-day compressive strength of the slab concrete, MPa,
ϕ_0 – the initial diameter of the bar, mm,
t – time, year,
α = 3 to 15– (accepted for calculations α = 3) relation between the homogenous corrosion penetration P_x and P_{pit} the maximum depth of a pit,
η = 1.73 to 2.87 – (accepted for calculations η = 1.73) corrosion rate, %,
V_{corr} – average corrosion rates (30 μm/year are given for the exposure classes XD2 or XD3 of EN206 [9]).

The drop in the prestressing force takes place when shear stresses at side surfaces of the prestressing tendons are higher than bond stresses (6), which will be observed after time $t_{cor.red}$ which should be greater than the time t_n, in which chloride ions will cover the whole group of tendons. As there are no relevant studies, we may expect two mechanisms of a drop in the prestressing force. The first mechanism- the rapid mechanism, is applicable if the bond loss occurs simultaneously along the side surfaces of all tendons. The second, and a more probable mechanism, is relevant if corrosion develops and covers other tendons. Then, a drop in prestressing force will be caused by bond loss and will depend on time, after which the degradation of bond stresses occurs according to the expression

$$\Delta P_{cor}\left(t > t_{cor.red}\right) = 4\tau_p(t)\sum_i \frac{A_{\phi 0i}}{\phi_{0i}} \cdot L\,, \tag{8}$$

The decrease in adhesion stresses occurs from $t_{\mathrm{cor.red}}$ to $t_{\mathrm{n.0}}$. The component related to the reduced area of prestressing tendons due to pitting corrosion, can be replaced with the uniform change of bar diameter used in case of common steel. In that case, the change in tendon area can be expressed as

$$\Delta A_{p.cort}\left(t > t_{ini.cor}\right) = \frac{\pi\phi_0^2\left(1 - 8.61\cdot 10^{-3} t\right)^2}{4}\,. \tag{9}$$

After time $t > t_{\mathrm{cor.max}}$, stress values in tendons can reach the design yield strength f_{pd}.

$$\frac{P_{m0} - \Delta P_{c+s+r}\left(t > t_{ini.cor}\right) - \Delta P_{cor}\left(t > t_{cor.red}\right)}{A_p - \Delta A_{p.cort}\left(t > t_{ini.cor}\right)} = f_{pd}\,. \tag{10}$$

Then, the change in tendon area would not cause the loss in bond strength, but increased values of stresses in tendons.

Taking into account the above, we modelled changes in prestressing force over time, for neglected and assumed effects of Cl^- ingress, and the results are presented in Table 1. As a comparative time, we used the planned operational period of the structure $t_{\mathrm{cor.red}}$ calculated according to the formula (9). The standard time of use of plates equal to 50 years is assumed.

Table 1. Calculated results

conditions	P_0 kN	t_0 day	t_u day	P_{m0} kN	$t_{ini,cor}$ year	t_n year	$t_{cor.red}$ year	$t_{n.0}$ year	$t_{cor.max}$ year	ΔP_{cor} kN/yr	P_{mt} kN
without the impact of Cl^-	1879	2	7	1685	--	--	--	--	--	--	1544.1 t =50 yr
with the impact of Cl^-					22	28	38.8	39.2	90	139.5	--

Time, after which corrosion in the tendons was initiated, was $t_{\mathrm{ini.cor}}$ = 22 years and the time after which the whole thick of the lower tendons was covered with chloride ions was t_n = 28 years. From that moment, bond stress was decreased τ_p. In time $t_{\mathrm{cor.red}}$ = 38.8 years, bond stresses reached the design bond stress f_{bpt} which caused the loss in prestressing force ΔP_{cor} = 139.5 kN/yr. The time after which the prestressing force has dropped to zero, causing the destruction of the element was $t_{\mathrm{n.0}}$ = 39.2 years. Reinforcement corrosion developing since time $t_{\mathrm{ini.cor}}$ reduced the area of prestressing tendons in such a way that prestressing force caused the tendons reached the design yield strength f_{pd}, after time $t_{\mathrm{cor.max}}$ = 90 years.

4. Conclusions

Static analyses of chloride ion effects indicate that the following consequences can occur:

- losses in prestressing forces can cause a rapid drop in a prestressing force, increased deflections and a formation of cracks that warn against failure. The second, less predictable mechanism, caused by pitting corrosion, can cause a rapid increase of stresses in tendons resulting in slab fracture without prior warning,
- on the basis of empirical data from the literature, which express the relationship between strength/bond over time, we determined the safe operational time $t_{\mathrm{cor.red}}$ = 38.8 years,

- the determined operational time that takes into account the effect of chloride ions is much shorter than time at the design stage, which was 50 years.

Further tests should focus on:

- determining close correlations between adhesion and concentration of Cl^- ions,
- specifying changes in the area of tendons caused by pitting corrosion,
- detailed description of relationships for proper determining losses in prestressing, which are caused by bond strength loss, changes in elasticity modulus of concrete, and the formation of corrosion products.

References

[1] A. Ajdukiewicz, J. Mames, Konstrukcje z betonu sprężonego [Prestressed concrete structures]. PC, 2004 (in Polish).
[2] U. Nürnberger, "Corrosion induced failures of prestressing steel" Otto-Graf-J. Vol. 13, 2002
[3] Y.C. Ou, Y. T. T. Susanto, H. Roh, "Tensile behavior of naturally and artificially corroded steel bars" Constr. Build. Mater.103: 93–104, 2016.
[4] B.Y. Lee, K. T. Koh, M. A. Ismail, H. S. Ryu, S. J. Kwon, "Corrosion and Strength Behaviors in Prestressed Tendon under Various Tensile Stress and Impressed Current Conditions" Adv. in Mater. Sci. and Eng., 7 pages, 2017
[5] F. Li, Y. Yuan, Ch. Q. Li, "Corrosion propagation of prestressing steel strands in concrete subject to chloride attack" Constr. Build. Mater. 25: 3878–3885, 2011.
[6] Y. Zhao, Y. Dou, "Study on Fatigue Damage Law of Bonding between Steel Strand and Concrete under Corrosive Environment of Chloride. Chem. Eng. Trans. 62, 1033-1038, 2017.
[7] F. Li, Y. Yuan, „Effects of corrosion on bond behavior between steel strand and concrete", Constr. Build. Mater. 38: 413–422, 2013.
[8] I. Martinez, C. Andrade "Examples of reinforcement corrosion monitoring by embedded sensors in concrete structures. Cement & Concrete Composites, 31, 2009, str. 545-554.
[9] PN-EN 206-1: 2003 Concrete. Part 1: Specification, performance, production and conformity.
[10] K. Stanish, R. D. Hooton, S. J. Pantazopoulou. "Corrosion Effects on Bond Strength in Reinforced Concrete" ACI Structural Journal, 915-922, 1999
[11] Z. Szweda, "Analysis of protective features of concrete in precast prestressed floor slabs (HC type) against chloride penetration", 8th Scientific-Technical Conference Material Problems in Civil Engineering (MATBUD'2018). (to be published)
[12] G. Troszczyński „Wytyczne projektowania stropów z płyt sprężonych „HC". Poradnik dla projektantów". [Guidelines for designing floors from prestressed slabs HC. Guidebook for designers.] FABUD WKB. S.A 2018, (in Polish).
[13] PN-ISO 9297: Determination of chlorides. Titration method with silver nitrate in the presence of chromate as indicator (Mohr Method).
[14] Z. Szweda, A. Zybura "Theoretical model and experimental tests on chloride diffusion and migration processes in concrete". Procedia Eng., 57: 1121-1130. 2013.
[15] Z. Szweda, "Resistance of concrete with ordinary and low-alkali Portland cement to chloride ingress". O. p. K. 5:148-153, 2016.
[16] Z. Szweda, T. Ponikiewski, J. Katzer, "A study on replacement of sand by granulated ISP slag in SCC as a factor formatting its durability against chloride ions". J. of Cl. Prod., 156:569-576, 2017.
[17] PN-EN 1992-1-1 Eurocode 2 - Design of concrete structures - Part 1-1
[18] Szweda Z., Śliwka A., "Predicting risk of corrosion of bridges made of concrete with portland cement and low alkali portland cement", The 12th Central European Congress on Concrete Engineering CCC 2017, Tokaj, Hungary, 118-126, 2017
[19] Szweda Z., Śliwka A., "Increasing load-bearing capacity of bridge structures by reducing cover thickness as a result of changing cement type", Procedia Eng. 193: 417–422. (2017)